

## A PRELIMINARY PANEL FLUTTER ANALYSIS FOR THE VLS PAYLOAD FAIRING

**José Guido Damilano**

**João Luiz F. Azevedo**

Centro Técnico Aeroespacial, Instituto de Aeronáutica e Espaço  
CTA/IAE/ASE – 12228-904 – São José dos Campos, SP, Brasil

**Abstract.** *The paper describes panel flutter analyses performed in the context of the development of the first Brazilian satellite launcher (VLS). The development of the structural-dynamic and aerodynamic formulations are presented, together with their coupling to obtain the aeroelastic equations. Two different approaches were used to describe the aerodynamic loading, namely formulations based on the quasi-steady, linearized, small perturbation potential equation and on 1st-order piston theory. Results are presented for the VLS main aerodynamic fairing panels, both at zero incidence and at angle of attack. The effect of the inclusion of the unsteady aerodynamic terms in the aeroelastic results was also investigated. The overall conclusion of the study indicates that the VLS payload shroud would be free from panel flutter even with a considerable reduction in the fairing panel thickness.*

**Keyw ords:** *VLS, Panel flutter, Piston theory, Payload fairing, Launch vehicles.*

### 1. INTR ODUCTION

The present work is concerned with panel flutter analyses performed in the context of the development of the first Brazilian satellite launcher, the VLS system. The VLS is a four-stage vehicle in which the first stage is composed of four strap-on boosters around a central core. The vehicle has a hammerhead-type payload shroud which is a configuration known to be prone to flow separation during the transonic or supersonic flight regimes. This observation, therefore, also indicates that considerably higher structural loads could be present over the payload fairing for these flight conditions. A schematic representation of the VLS system is presented in Fig. 1. The vehicle is being designed for the mission of launching small satellites, of the order of 150 to 200 kg, into low Earth orbit (LEO). Moreover, this vehicle is an integral part of a larger program which has the goal of launching a Brazilian satellite, using a Brazilian-built rocket, from a Brazilian launching site. The satellite development is the responsibility of Instituto Nacional de Pesquisas Espaciais (INPE) whereas the launching site is the Alcântara Launching Complex (CLA). The responsibility of designing and building the launcher itself falls with Instituto de Aeronáutica e Espaço (IAE) which, together with its industrial partners, should deliver the VLS ready for launch.

The vehicle has been under development for a few years now and, recently, there was an intensive effort to try to finalize its aeroelastic clearance studies. In particular, as in the development of any satellite launcher, panel flutter analyses are an important issue to be considered.

Moreover, it is correct to state that aeroelastic considerations were not taken into account in the original design studies and structural sizing of the vehicle. These considerations were treated as afterwards verifications, which is also a fairly common procedure in many organizations. The aspects which were mainly emphasized in the VLS aeroelastic clearance studies were transonic buffeting for the central body payload shroud, classical flutter and divergence of the vehicle fins, panel flutter and vortex shedding at takeoff conditions. It should be emphasized that the final

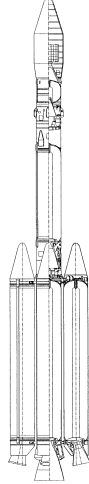


Figure 1: Sketch of the VLS system.

VLS configuration, as shown in Fig. 1, does not have fins in the first stage boosters. However, until recently, the primary configuration under study was supposed to have those fins and there is no guarantee that future vehicle upgrades will not require the fins.

The present paper describes one of these studies, namely the verification of panel flutter stability for the vehicle main aerodynamic fairing, i.e., the payload shroud. The initial studies for the VLS design indicated that the payload shroud would be made with composite materials. For several reasons, which are beyond the scope of the present paper, there was a decision to use standard aeronautical construction for the fairing. Hence, it currently has several longerons and stiffeners which are riveted to the aluminum skin. Stiffeners and longerons are also made of aluminum. The overall fairing construction allows its modeling as composed of several rectangular patches supported at the longerons and stiffeners. The flat patches are uniform, isotropic, thin and simply supported on the four edges. The aerodynamic loading is based on the two-dimensional “static approximation” in the first instance including the effect of yaw of the panel. Then, unsteady terms are included in the aerodynamic formulation. The approximate solution is obtained by using Lagrange’s equations and oblique coordinates. Numerical results indicate that, even at the maximum dynamic pressure flight condition and if the plate thickness were reduced in half, the flutter dynamic pressure would still be considerably higher than the actual flight dynamic pressure.

## 2. STRUCTURAL FORMULATION

The parallelogrammic flat panel simply supported all around is assumed to be uniform, thin, and isotropic. Damping is neglected and the classical, small-deflection, thin-plate theory is used in the structural formulation. The effect of yaw of the parallelogrammic panel is taken into account. Lagrange’s equations are used to derive the equations of motion of the approximate solution. The potential energy of the system is written based on the strain energy of deformation of the plate and the work of the mid-plane forces. The panel is exposed to supersonic flow on one side and to still air on the other. Figure 2 shows the geometry of the panel, the system of

oblique coordinates and the aerodynamic flow. The use of the classical small-deflection theory allows the governing equation for the problem to be written as

$$D\nabla^4 W + N_x W_{,xx} + 2N_{xy} W_{,xy} + N_y W_{,yy} + \rho h W_{,tt} = \ell(x, y, t), \quad (1)$$

where  $D = Eh^3/12(1-\nu^2)$  is the stiffness of the plate,  $\nabla^4$  is the biharmonic operator in oblique coordinates,  $\rho$  is the mass density of the material,  $h$  and  $W$  are the thickness and transverse displacement of the panel, respectively, and  $\ell(x, y, t)$  is the aerodynamic loading normal to the middle plane of the panel. Moreover,  $N_x$ ,  $N_{xy}$  and  $N_y$  represent the structural loading at the mid-plane of the plate. Subscripts after a comma denote differentiation. The boundaries of

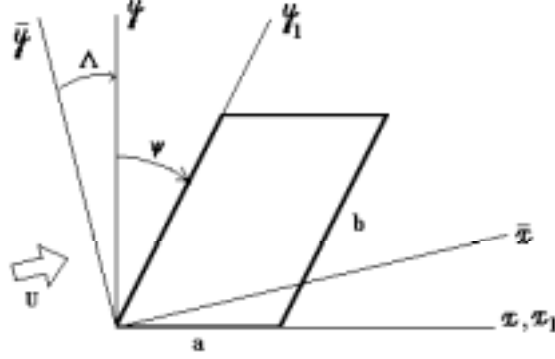


Figure 2: Parallelogramic panel and oblique coordinate system for the panel in yaw.

the panel, in oblique coordinates, are  $x_1 = 0$ ,  $x_1 = a$ ,  $y_1 = 0$  and  $y_1 = b$ . The rectangular coordinates and the oblique coordinates are related by the expressions  $x_1 = x - y \tan \Psi$  and  $y_1 = y \sec \Psi$ , where  $\Psi$  is the angle of skew of the panel.

### 3. AEROELASTIC FORMULATION

The aeroelastic equations for the problem are derived using two aerodynamic theories. The first one considers a quasi-steady aerodynamic formulation based on the linearized small perturbation potential equation. The second one uses a 1st-order piston theory which includes unsteady aerodynamic effects.

#### 3.1 Quasi-steady aerodynamic formulation

The equations of motion of the system are obtained by the use of Lagrange's equations

$$\frac{d}{dt} \left( \frac{\partial T}{\partial \dot{q}_i} \right) - \frac{\partial T}{\partial q_i} + \frac{\partial U}{\partial q_i} = Q_i(t), \quad i = 1, 2, \dots, k. \quad (2)$$

The kinetic energy is given by

$$T = \frac{1}{2} \cos \Psi \int_0^b \int_0^a \rho h \dot{W}^2 dx_1 dy_1. \quad (3)$$

From thin-plate theory, the potential energy of the system  $U$  consisting of the strain energy of deformation of the plate expressed in oblique coordinates and the work of the mid-plane forces is given by

$$\begin{aligned} U &= \frac{D}{2} \cos \Psi \int_0^b \int_0^a [(\nabla^2 W)^2 - 2(1-\nu) \sec^2 \Psi (W_{,x_1 x_1} W_{,y_1 y_1} - W_{,x_1 y_1}^2)] dx_1 dy_1 \\ &- \frac{1}{2} \cos \Psi \int_0^b \int_0^a [N_x W_{,x_1}^2 + N_y \sec^2 \Psi (W_{,y_1} - \sin \Psi W_{,x_1})^2 \\ &+ 2N_{xy} \sec \Psi W_{,x_1} (W_{,y_1} - \sin \Psi W_{,x_1})] dx_1 dy_1, \end{aligned} \quad (4)$$

where  $\nabla^2 W = \sec^2 \Psi (W_{,x_1 x_1} - 2 \sin \Psi W_{,x_1 y_1} + W_{,y_1 y_1})$  is the Laplacian in oblique coordinates applied to  $W$ . The quasi-steady aerodynamic loading, based on the linearized small perturbation potential equation (Bisplinghoff, Ashley and Halfman, 1955, and Liepmann and Roshko, 1957) is given by

$$\ell(x, y, t) = -\frac{2q}{\beta} \left( \frac{\partial W}{\partial x} \right) \quad (5)$$

where  $q = \frac{1}{2} \rho_a \mathcal{U}^2$  is the dynamic pressure,  $\rho_a$  and  $\mathcal{U}$  are, respectively, the air density and the mean flow velocity, and  $\beta = \sqrt{M^2 - 1}$ , with  $M$  denoting the freestream Mach number.

The deflection of the panel can be written as

$$W(\xi, \eta, t) = \sum_{i=1}^k q_i(t) \phi_i(\xi, \eta), \quad (6)$$

where  $\xi = x_1/a$  and  $\eta = y_1/b$  are nondimensional oblique coordinates. Thus, the kinetic and strain energies expressions can be rewritten, respectively, as

$$T = \frac{1}{2} \sum_{i=1}^k \sum_{j=1}^k m_{ij} \dot{q}_i \dot{q}_j \quad \text{and} \quad U = \frac{1}{2} \sum_{i=1}^k \sum_{j=1}^k k_{ij} q_i q_j, \quad (7)$$

where  $m_{ij}$  and  $k_{ij}$  are presented in Durvasula (1966).

Taking into account the effect of yaw of the parallelogramic panel, as shown in Fig. 2, the aerodynamic loading, considering a quasi-steady formulation based on the linearized small perturbation potential equation, is written, in normalized oblique coordinates, as

$$\ell(\xi, \eta, t) = \frac{-2q}{a\beta} [(\cos \Lambda - \sin \Lambda \tan \Psi) W_{,\xi} + \frac{a}{b} \sin \Lambda \sec \Psi W_{,\eta}] \quad (8)$$

where  $\Lambda$  is the angle between the flow direction and the axis  $x$  (yaw angle). The generalized forces  $Q_i(t)$  can be calculated considering the virtual work of the aerodynamic loading as:

$$\begin{aligned} \delta \bar{W} = Q_i(t) \delta q_i = & - \frac{2qb \cos \Psi}{\beta} \int_0^1 \int_0^1 [(\cos \Lambda - \sin \Lambda \tan \Psi) W_{,\xi} \\ & + \frac{a}{b} \sin \Lambda \sec \Psi W_{,\eta}] \delta W d\xi d\eta \end{aligned} \quad (9)$$

from which one can write:

$$Q_i = -\frac{2qb \cos \Psi}{\beta} \sum_{j=1}^k L_{ij} q_j, \quad (10)$$

where

$$L_{ij} = \int_0^1 \int_0^1 [(\cos \Lambda - \sin \Lambda \tan \Psi) \phi_{j,\xi} + \phi_{j,\eta} \frac{a}{b} \sin \Lambda \sec \Psi] \phi_i d\xi d\eta.$$

Substituting the expressions for the kinetic energy  $T$ , strain energy  $U$  and generalized forces  $Q_i$  into the Lagrange's equations (2), one can write

$$[\tilde{M}]\{\ddot{q}\} + [\tilde{K}]\{\dot{q}\} = [\tilde{L}]\{q\}. \quad (11)$$

At the critical flutter condition, as the motion is simple harmonic, the modal deformations can be written

$$\{q\} = Re\{C_i\} e^{i\omega t}, \quad (12)$$

where  $\{C_i\}$  is the vector of constants to be determined and  $\omega$  is the frequency of oscillation. Substituting this equation into Eq. (11) the resulting system of algebraic homogeneous equations is

$$[[\tilde{K}] - \omega^2 [\tilde{M}] - [\tilde{L}]]\{C\} = \{0\}. \quad (13)$$

For the simply supported panel, the boundary conditions are  $W = 0$  and  $M_n = 0$  all along the boundary. For the polygonal boundary, the foregoing boundary conditions reduce to  $W = 0$  and  $\nabla^2 W = 0$  on the boundary. For the assumed displacement mode function  $\phi_i$  one can take

$$\phi_i(\xi, \eta) \sim \phi_{mn}(\xi, \eta) = \sin m\pi\xi \sin n\pi\eta, \quad \text{with} \quad \begin{cases} m = 1, 2, \dots, \mathcal{M} \\ n = 1, 2, \dots, \mathcal{N} \end{cases} \quad (14)$$

and also, accordingly,  $k_{ij} \sim k_{mnrst}$ ,  $m_{ij} \sim m_{mnrst}$ ,  $Q_i \sim Q_{mn}$  and  $L_{ij} \sim L_{mnrst}$ . Thus, Eq. (13) can be rewritten as

$$[E_{mnrst}]\{C_{rs}\} = \bar{k}^{*2}\{C_{rs}\} \quad (15)$$

where  $\bar{k}^{*2} = \frac{\rho h a^4 \cos^4 \Psi}{D \pi^4} \omega^2$  and  $[E_{mnrst}]$  is defined in Damilano and Azevedo (1998). Also, the dynamic pressure parameter, present in  $[E_{mnrst}]$ , is given by  $Q^* = \frac{2q a^3 \cos^4 \Psi}{\beta D \pi^4}$ .

The matrix equation (15) corresponds to the general flutter problem of a parallelogrammic panel simply supported all around acted upon by uniform in-plane loads  $N_x$ ,  $N_y$ , and  $N_{xy}$ . This work, however, is concerned with the panel flutter of unstressed panels, i.e., with  $N_x$ ,  $N_y$ , and  $N_{xy}$  all equal to zero. The eigenvalues  $\bar{k}^{*2}$  of the matrix  $[E_{mnrst}]$  represent the frequencies of vibration of the panel. For the static aerodynamic theory used, all eigenvalues of  $[E_{mnrst}]$  are real for sufficiently small values of  $Q^*$ . Actually, for  $Q^* = 0$ , Eq. (15) refers to a free vibration problem and the resulting eigenvalues correspond to the in vacuo frequencies of the panel. Gradually increasing  $Q^*$ , some eigenvalues approach each other and, for a certain value of  $Q^*$ , two roots coalesce forming an eigenvalue loop. Further increasing the value of  $Q^*$ , these two roots become complex. When the roots  $\bar{k}^{*2}$  become complex, the corresponding motion clearly is a divergent oscillation. Thus, the value of  $Q^*$  at which two eigenvalues coalesce defines the critical value  $Q_{cr}^*$  for flutter.

### 3.2 Aerodynamic formulation with piston theory

The aerodynamic loading, considering first order piston theory (Ashley and Zartarian, 1956), can be written as

$$\ell(x, y, t) = - \left( \frac{2q}{M} \right) \left( \frac{1}{U} \frac{\partial W}{\partial t} + \frac{\partial W}{\partial x} \right). \quad (16)$$

The structural-dynamic formulation is still given by Eq. (1). Hence, the aerodynamic loading, rewritten in terms of the dimensionless coordinates and considering the coordinate system indicated in Fig. 2, can be expressed as

$$\ell(\xi, \eta, t) = - \frac{2q}{aM} \left[ (\cos \Lambda - \sin \Lambda \tan \Psi) W_{,\xi} + \frac{a}{b} \sin \Lambda \sec \Psi W_{,\eta} + \frac{a}{U} W_{,t} \right]. \quad (17)$$

The  $Q_i(t)$  generalized forces, obtained from the virtual work performed by the aerodynamic forces, can be written in this case as

$$Q_i(t) = - \frac{2qb \cos \Psi}{M} \left( \sum_{j=1}^k L_{1,ij} q_j + \sum_{j=1}^k L_{2,ij} \dot{q}_j \right), \quad (18)$$

where

$$\begin{aligned} L_{1,ij} &= \int_0^1 \int_0^1 \left[ (\cos \Lambda - \sin \Lambda \tan \Psi) \Phi_{j,\xi} + \frac{a}{b} \sin \Lambda \sec \Psi \Phi_{j,\eta} \right] \Phi_i d\xi d\eta, \\ L_{2,ij} &= \int_0^1 \int_0^1 \frac{a}{b} \Phi_j \Phi_i d\xi d\eta. \end{aligned} \quad (19)$$

The equations describing the motion of the panel in terms of the modal coordinates can be obtained, using Lagrange's equations of motion, as

$$[\tilde{M}] \{\ddot{q}\} + [\tilde{K}] \{q\} = [\tilde{L}_1] \{q\} + [\tilde{L}_2] \{\dot{q}\}. \quad (20)$$

The present formulation does not allow a direct eigenvalue analysis, as performed in the previous case, due to the presence of the modal velocities in Eq. (20). If one considers the transformation of variables defined by  $q_1 = q$  and  $q_2 = \dot{q}$ , it is possible to rewrite the equations of motion in a standard first-order form as

$$\begin{Bmatrix} \dot{q}_1 \\ \dot{q}_2 \end{Bmatrix} = \begin{bmatrix} [0] & [I] \\ [\tilde{L}'_1] - [\tilde{K}'] & [\tilde{L}'_2] \end{bmatrix} \begin{Bmatrix} q_1 \\ q_2 \end{Bmatrix}. \quad (21)$$

The various matrix terms in Eq. (21) were obtained from the matrices in Eq. (20) after appropriate normalizations. The interested reader is referred to Said, Azevedo and Damilano (1998) for further details of this derivation. It is also possible to show (Said, Azevedo and Damilano, 1998) that these terms can be written as

$$\begin{aligned} [\tilde{L}'_2] &= -\frac{a_\infty \rho_a}{h \rho} [I], \\ [\tilde{L}'_1] - [\tilde{K}'] &= -\frac{D}{a^4 \rho h \cos^4 \Psi} [E_{mnrst}], \end{aligned} \quad (22)$$

where  $[E_{mnrst}]$  appeared originally in Eq. (15). If one considers that, at the critical flutter condition, the motion is of the form

$$\{q\} = \text{Re}\{C_i\} e^{\omega t}, \quad (23)$$

it is again possible to perform an eigenvalue-based stability analysis for the system. In this case, the instability condition will be reached when the real part of any of the eigenvalues becomes positive, since this will yield an exponentially growing amplitude of motion.

#### 4. SOME VALIDATION RESULTS

The formulation described in Section 3.1 was validated based on numerical (Durvasula, 1966) and analytical (Dowell, 1975) solutions, whereas the formulation presented in Section 3.2 was partially validated, based on the same examples, however taking the terms of matrix  $[\tilde{L}_2]$  equal to zero.

An evaluation of the effect of the unsteady aerodynamic terms present in the 1st-order piston theory formulation was also performed. Results in graphical form are not presented here for the sake of brevity. However, the calculations indicated that, all other parameters held fixed, the lowest values of  $Q_{cr}^*$  correspond to the results obtained without including the unsteady terms, i.e., using quasi-steady aerodynamics. Moreover, computations with 1st-order piston theory used two different values of freestream air density, namely  $\rho_a = 0.600 \text{ kg/m}^3$  and  $1.228 \text{ kg/m}^3$ . The results indicated that higher values of air density yield larger values of  $Q_{cr}^*$ . Therefore, the conclusion of these analyses is that, for the present cases, the inclusion of unsteady effects increases the flutter dynamic pressure because the unsteady aerodynamic terms add damping to the system. Moreover, higher air densities yield larger damping effects which, in turn, further increase the flutter dynamic pressure.

The results for a flutter analysis using 1st-order piston theory and considering a panel with  $a/b = 1$ , with air density  $\rho_a = 1.228 \text{ kg/m}^3$  and  $\Lambda = 0 \text{ deg.}$ , are presented in Fig. 3 in terms of the root locus of the first eigenvalue that becomes unstable. One can observe that, as  $Q^*$  is increased, initially the real part of the eigenvalue is essentially constant. Further increase in  $Q^*$  makes the real part of the eigenvalue move towards the unstable right-hand semi-plane and, at  $Q_{cr}^* = 5.9$ , there is the onset of flutter for this case.

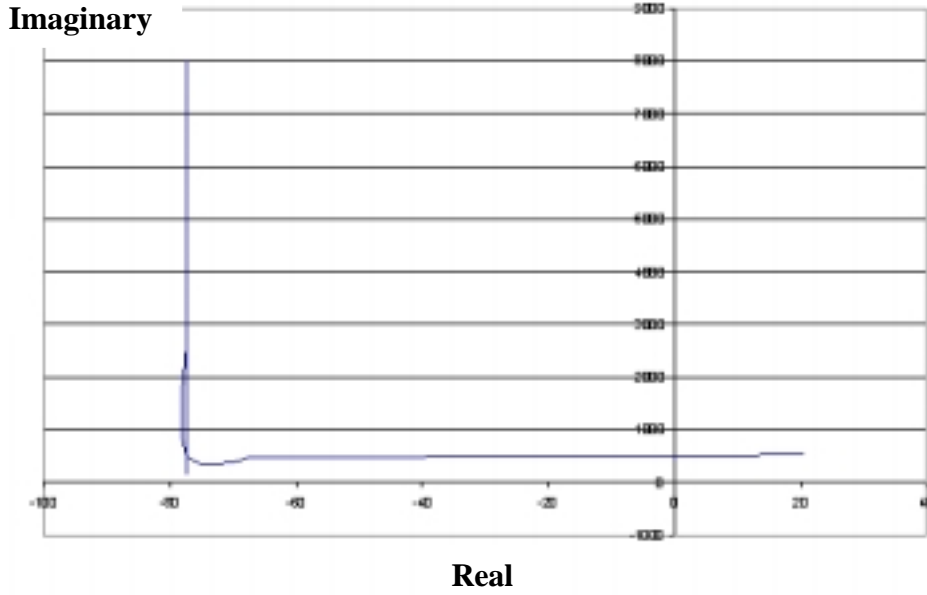


Figure 3: Root locus for the first eigenvalue that becomes unstable with  $N_x = N_y = N_{xy} = 0$  and  $\Psi = \Lambda = 0$ .

## 5. FLUTTER ANALYSES FOR THE VLS MAIN FAIRING

A typical panel was chosen from the cylindrical region of the VLS main fairing for the analyses. The rectangular panel is simply supported all around the boundary. The elastic deformations of the support, i.e., the elastic deformations of the longerons and stiffeners, were neglected. The panel to be analyzed is rectangular with  $a = 115$  mm and  $b = 120$  mm. For the work herein described, firstly a yaw angle of 0 deg. was used. Since the chosen typical panel has sides parallel to the axes of the coordinate system, thus  $\Psi = 0$  deg. too. The calculations were performed using 16 term series by taking  $\mathcal{M} = 4$  and  $\mathcal{N} = 4$ , and with the mid-plane loads  $N_x = N_y = N_{xy} = 0$ . The results, pictured in Fig. 4, showed coalescence between the 1st and 2nd frequencies for  $Q_{cr}^* = 5.11$ . If the vehicle flies with angles of attack different from zero, it would be equivalent to having the side panels with angle of yaw,  $\Lambda$ , with respect to the flow, also different from zero. In the VLS case, all along its trajectory, the angle of attack varies from 0 to 6 deg. As shown in the literature (Durvasula, 1966), and confirmed by the results obtained, the existence of yawing angles, in the range of 0 to 10 deg., when  $\Psi = 0$  deg. and  $a/b = 1$ , typically leads to higher critical flutter dynamic pressures. Thus, the results obtained for  $\Lambda = 0$  were considered in the study described as follows. The panel's material is aluminum with  $E = 70$  GPa,  $\nu = 0.3$ , and thickness  $h = 1.0$  mm. It is possible to write  $q/\beta$  as function of  $Q^*$  by using the expression

$$\frac{q}{\beta} = \frac{\pi^4 E}{24a^3(1-\nu^2)\cos^4\Psi} Q^* h^3. \quad (24)$$

Then, substituting the value obtained for  $Q_{cr}^*$  into Eq. (24) results  $q/\beta = 1.05 \times 10^6 \text{N/m}^2$ . From the vehicle's flight data (Many authors, 1991) at time  $t = 42$  s, the maximum dynamic pressure is  $q_{max} = 9.28 \times 10^4 \text{N/m}^2$  corresponding to a Mach number  $M = 2.383$ , which results in  $q/\beta = 4.29 \times 10^4 \text{N/m}^2$ . The results clearly indicate a very safe vehicle operation, as far as panel flutter is concerned, since  $q/\beta$ , for the critical dynamic pressure parameter of the vehicle, is almost 2 orders of magnitude larger than the actual value obtained with the vehicle flight data. Moreover, if the panel thickness is reduced to 0.5 mm, the previous numerical procedures will produce  $q/\beta = 1.31 \times 10^5 \text{N/m}^2$ , which still represents a very stable condition, since the result is about 3 times larger than the one that actually occurs during the flight of the vehicle.

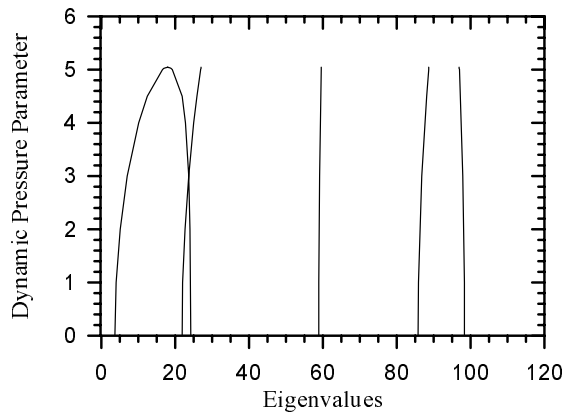


Figure 4: Eigenvalues as function of the aerodynamic loading  $Q^*$ .

Another approach to present the previously discussed results would be to plot the stability region for the VLS main fairing for a fixed flight dynamic pressure, and as a function of the flight Mach number and panel thickness. This is indicated in Fig. 5 for the case in which the aerodynamic forces are calculated using the quasi-steady, small disturbances potential theory. All the geometric and material data used in this case are the same as in the previous discussion. For the present calculations, however, the point along the vehicle trajectory corresponding to 35 s after liftoff was considered, which yields a freestream dynamic pressure of  $78.3 \times 10^3 \text{ N/m}^2$ . The points above the curve in Fig. 5 correspond to stable operation as far as panel flutter is concerned, whereas those below the curve are unstable points.

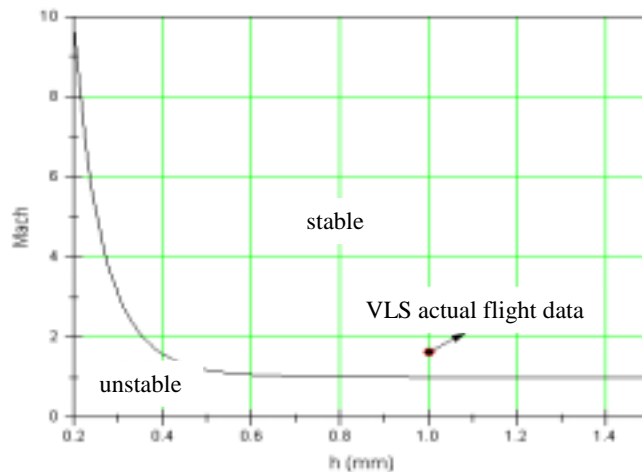


Figure 5: Stability region for the VLS payload shroud panels calculated using quasi-steady aerodynamics ( $q = 78.3 \times 10^3 \text{ N/m}^2$ ).

The actual point corresponding to the VLS payload shroud panels in the above conditions is also indicated in Fig. 5. One can see that this point is well within the stable region. Moreover, one can also observe that, all other parameters remaining constant, the panel thickness could be reduced to approximately 0.4 mm without the occurrence of panel flutter for this flight condition.

Similar results are presented in Fig. 6, but for the aerodynamic loads computed using 1st-



order piston theory. As before, all other parameters and the flight dynamic pressure are held

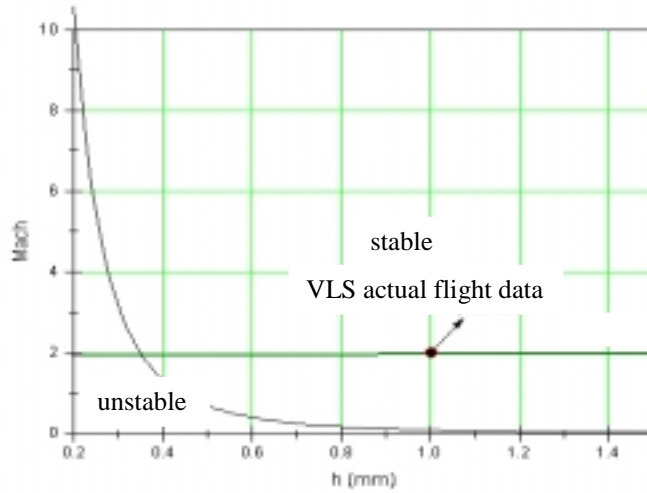


Figure 6: Stability region for the VLS payload shroud panels calculated using 1st-order piston theory ( $q = 87.0 \times 10^3 \text{ N/m}^2$ ,  $\rho_a = 0.447 \text{ kg/m}^3$  and altitude = 9375 m).

fixed, whereas the Mach number and panel thickness are varied in order to determine the flutter stability limit. The dynamic pressure was fixed at  $87.0 \times 10^3 \text{ N/m}^2$  in this case, which corresponds to flight at 40 s after liftoff for the VLS nominal trajectory. Again, the actual point corresponding to the VLS flight at this condition is also shown in Fig. 6, and one can observe that the vehicle is clearly stable for panel flutter under such conditions. The dimensionless critical flutter dynamic pressure at this condition, calculated using piston theory, is  $Q_{cr}^* = 5.16$ . For the same conditions, if the flutter limit were computed using quasi-steady aerodynamics, the calculation would yield  $Q_{cr}^* = 5.11$ . This behavior is in agreement with the results previously discussed, since the addition of the unsteady terms adds damping to the system and, hence, increases the flutter speed.

A still different form of trying to summarize the results of the present investigation is shown in Fig. 7. In this case, the panel thickness was held fixed at  $h = 0.5 \text{ mm}$ , and the dynamic

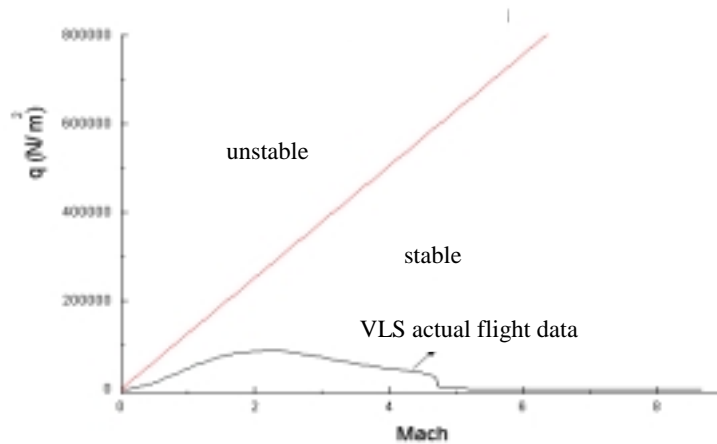


Figure 7: Comparison of flutter dynamic pressure and actual flight dynamic pressure along the VLS nominal trajectory for payload shroud panel thickness assumed as 0.5 mm.

pressure for the flutter stability limit was calculated as a function of the flight Mach number. All geometric and material parameters are equal to the values used in the previous analyses for

the VLS, and the atmospheric data is taken, as a function of the flight Mach number, from the vehicle nominal flight trajectory. The panel thickness was considered at half of its actual value for the VLS panels because the authors wanted to emphasize that, even with such a drastic reduction on the fairing plate thickness, the vehicle was still safe with regard to panel flutter. The actual flight dynamic pressure for the VLS, as a function of Mach number, is also shown in Fig. 7 for comparison purposes. It is clear from this figure that the panel flutter margin for the payload shroud panels is very large throughout the relevant portion of the flight trajectory, even with half the actual plate thickness. The quasi-steady aerodynamic formulation was used for the calculations presented in Fig. 7.

## 6. CONCLUSIONS

Panel flutter analyses were performed in the context of the development of the first Brazilian satellite launcher (VLS). Lagrange's equations were used to derive the aeroelastic equations for the problem. The aerodynamic loading was obtained based on two different aerodynamic formulations, namely the quasi-steady linearized small perturbation equation and the 1st-order piston theory. The panels are considered flat, rectangular, isotropic, and simply supported all along the boundary. The numerical results obtained indicate that the VLS payload shroud should fly free from panel flutter even with a considerable reduction in the fairing panel thickness. Moreover, the results also indicated that the inclusion of unsteady aerodynamic terms in the formulation consistently increases the flutter dynamic pressure for the present cases. Future work will concentrate on the evaluation of the effect of the support flexibility in the overall panel flutter stability.

## Acknowledgments

The present work was partially supported by Conselho Nacional de Desenvolvimento Científico e Tecnológico, CNPq, under the Integrated Project Research Grant No. 522413/96-0.

## REFERENCES

- Ashley, H., and Zartarian, G., 1956, Piston theory – a new aerodynamic tool for the aeroelastician, *Journal of the Aeronautical Sciences*, Vol. 23, No. 12, pp. 1109-1118.
- Bisplinghoff, R. L., Ashley, H., and Halfman, R. L., 1955, *Aeroelasticity*, Addison-Wesley, Cambridge.
- Damilano, J.G., and Azevedo, J.L.F., 1998, Aeroelastic analysis applied to the main fairing of the satellite launcher vehicle – VLS, Report RT-005/ASE-E/98, Space Systems Division, Instituto de Aeronáutica e Espaço, São José dos Campos, SP, Brazil (in Portuguese, original title is “Análise Aeroelástica Aplicada à Coifa Principal do Veículo Lançador de Satélites – VLS”).
- Dowell, E. H., 1975, *Aeroelasticity of Plates and Shells*, Noordhoff International Publishing Leyden.
- Durvasula, S., 1966, Flutter of simply supported, parallelogrammic, flat panels in supersonic flow, *AIAA Journal*, Vol. 5, No. 9, pp. 1668-1673.
- Liepmann, H. W., and Roshko, A., 1957, *Elements of Gasdynamics*, John Wiley, New York.
- Many authors, 1991, VLS database, Report No. 590-000000/B0004, Instituto de Aeronáutica e Espaço, São José dos Campos, SP, Brazil (in Portuguese).
- Said, J.C., Azevedo, J.L.F., and Damilano, J.G., 1998, Panel flutter studies for the VLS, Report NT-158/ASE-N/98, Space Systems Division, Instituto de Aeronáutica e Espaço, São José dos Campos, SP, Brazil (in Portuguese).